

Majorana mode leaking into a spin-charge entangled double quantum dot

Piotr Majek* and Ireneusz Weymann†
*Institute of Spintronics and Quantum Information,
 Faculty of Physics, Adam Mickiewicz University,
 ul. Uniwersytetu Poznańskiego 2, 61-614 Poznań, Poland*
 (Dated: October 5, 2021)

The signatures of Majorana zero-energy mode leaking into a spin-charge entangled double quantum dot are investigated theoretically in the strong electron correlation regime. The considered setup consists of two capacitively coupled quantum dots attached to external contacts and side-attached to topological superconducting wire hosting Majorana quasiparticles. We show that the presence of Majorana mode gives rise to unique features in the local density of states in the $SU(4)$ Kondo regime. Moreover, it greatly modifies the gate voltage dependence of the linear conductance, leading to fractional values of the conductance. We also analyze the effect of a finite length of topological wire and demonstrate that non-zero overlap of Majorana modes at the ends of the wire is revealed in local extrema present in the local density of states of the dot coupled directly to the wire. The calculations are performed with the aid of the numerical renormalization group method.

I. INTRODUCTION

One-dimensional topological superconductors or the chains of adatoms on superconducting substrates are promising platforms to realize Majorana zero-energy modes at the edges [1–6]. Signatures of such modes have already been reported by several experiments [7–19]. There is in fact a great interest in exploring the properties of such Majorana systems, due to expected applications in topological quantum computation [20–22]. Another important aspect making such hybrid systems interesting is related to the impact and signatures of the presence of Majorana modes in the transport properties of attached low-dimensional structures [13, 23–34]. In this regard, the leakage of Majorana zero-energy modes into attached quantum dots has been a subject of extensive investigations [35–38]. It was shown that the coupling to topological superconductor hosting Majorana quasiparticles (Majorana wire) results in fractional values of the conductance [35, 39]. Moreover, the transport properties of strongly correlated systems have also been explored in the context of interplay between the Kondo and Majorana physics [27, 39–46].

Here we make a further step in the understanding of the interplay between the Majorana zero-energy modes and strong electron correlations in the case of devices comprising coupled quantum dots. In particular, we explore the signatures of Majorana quasiparticles in the transport properties of spin-charge entangled double quantum dot (DQD), see Fig. 1, exhibiting the $SU(4)$ Kondo effect. Such Kondo effect results from the four-fold degeneracy of the ground state due to the orbital and spin degrees of the freedom [47–55], which can be achieved by appropriate tuning of the gate voltages [56, 57]. It is worthy of note that the transport proper-

ties of double dots attached to topological superconducting nanowires have already been studied [33, 45, 58–62]. However, the system’s behavior in the strongly-correlated regime is still rather unexplored. The goal of this paper is therefore to shed more light on this problem. To do so, we employ the nonperturbative numerical renormalization group (NRG) method [63], which allows us to accurately study the equilibrium transport properties of the system. We determine the relevant spectral functions and linear conductance through the system for various strengths of coupling to Majorana wire. We show that the presence of Majorana zero-energy modes gives rise to unique features visible in the local density of states of the double dot. Moreover, we study the gate voltage dependence of the conductance and predict its fractional values depending on the occupation of the quantum dot system. Finally, we also explore the impact of finite overlap of Majorana modes and show that it additionally modifies the behavior of both the local density of states and the conductance.

The paper is structured as follows. Section II is devoted to the theoretical formulation of the problem,

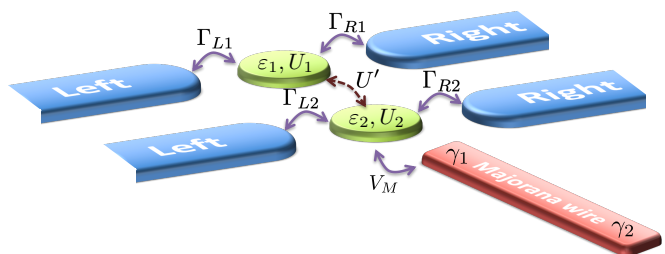


FIG. 1. The schematic of a double quantum dot coupled to a topological superconductor hosting Majorana zero-energy modes (Majorana wire). Each dot is characterized by its energy ϵ_j and Coulomb correlations U_j , while U' denotes the electron correlations between the dots. Every dot is connected to separate left and right leads with strength Γ_{rj} . The second dot is coupled to the Majorana wire (with amplitude V_M) hosting Majorana modes described by operators γ_1 and γ_2 .

* pmajek@amu.edu.pl

† weymann@amu.edu.pl

where the Hamiltonian and method are described. The main results and their discussion are presented in Sec. III, where we first discuss the behavior of the spectral function and then analyze the gate voltage and temperature dependence of conductance. The focus is on both the $SU(4)$ and $SU(2)$ Kondo regimes. The paper is summarized in Sec. IV.

II. THEORETICAL FORMULATION

The system consists of a double quantum dot attached to a topological superconducting wire hosting Majorana zero-energy modes at its ends, see Fig. 1. Each quantum dot is coupled to its own left and right electrode. The two dots are assumed to be capacitively coupled, while the hopping between the dots is negligible [57]. The Hamiltonian of the whole system is given by

$$H = H_{\text{leads}} + H_{\text{tun}} + H_{\text{MD}}, \quad (1)$$

where the first term describes the leads within the free quasiparticle approximation

$$H_{\text{leads}} = \sum_{r=L,R} \sum_{j=1,2} \sum_{\mathbf{k}\sigma} \varepsilon_{rj\mathbf{k}} c_{rj\mathbf{k}\sigma}^\dagger c_{rj\mathbf{k}\sigma}. \quad (2)$$

Here, $c_{rj\mathbf{k}\sigma}^\dagger$ is the creation operator of a spin- σ electron with momentum \mathbf{k} in the left ($r = L$) or right ($r = R$) lead attached to the first ($j = 1$) or second ($j = 2$) quantum dot, and $\varepsilon_{rj\mathbf{k}}$ is the corresponding energy. The second term of the Hamiltonian describes the tunneling process between double dot and the leads. It is given by

$$H_{\text{tun}} = \sum_{r=L,R} \sum_{j=1,2} \sum_{\mathbf{k}\sigma} v_{rj} \left(d_{j\sigma}^\dagger c_{rj\mathbf{k}\sigma} + c_{rj\mathbf{k}\sigma}^\dagger d_{j\sigma} \right), \quad (3)$$

where $d_{j\sigma}^\dagger$ creates an electron with spin σ on the j th dot and v_{rj} are the tunnel matrix elements between the dot j and lead r . The quantum dot level broadening is given by $\Gamma_{rj} = \pi \rho_{rj} v_{rj}^2$, where ρ_{rj} denotes the corresponding density of states. Finally, the Hamiltonian of the double dot attached to Majorana wire reads

$$H_{\text{MD}} = \sum_{j\sigma} \varepsilon_j d_{j\sigma}^\dagger d_{j\sigma} + \sum_j U_j d_{j\uparrow}^\dagger d_{j\uparrow} d_{j\downarrow}^\dagger d_{j\downarrow} + U' n_1 n_2 + \sqrt{2} V_M (d_{2\downarrow}^\dagger \gamma_1 + \gamma_1 d_{2\downarrow}) + i \varepsilon_M \gamma_1 \gamma_2, \quad (4)$$

where ε_j denotes the energy of an electron on dot j and U_j stands for the Coulomb correlation energy between two electrons occupying the same dot. The Coulomb correlations between the two quantum dots are denoted by U' , where $n_j = \sum_{\sigma} d_{j\sigma}^\dagger d_{j\sigma}$. It is assumed that the spin-down component of the second quantum dot is coupled to the Majorana wire with the amplitude V_M [23, 39, 42, 43, 45, 64]. The Majorana operators are denoted by γ_1 and γ_2 , respectively, and ε_M is the overlap between the Majorana zero-energy modes [12].

We are interested in the linear response transport properties of the system at low temperatures. To accurately resolve this transport regime, taking into account all electron correlations in a non-perturbative manner, we make use of the NRG method [63, 65, 66]. This approach allows for a very reliable calculation of various correlation functions of the system. In particular, we are interested in the behavior of the spectral function, which can be generally defined as $A(\omega) = -\text{Im}\{G^R(\omega)\}/\pi$, where $G^R(\omega)$ is the Fourier transform of the retarded Green's function $G^R(t) = -i\Theta(t)\langle\{O^\dagger(0), O(t)\}\rangle$, where O is an operator describing the double dot ($O = d_{j\sigma}$).

The linear response conductance through the quantum dot j flowing in the spin channel σ between the left and right contacts can be found from

$$G_{j\sigma} = \frac{e^2}{h} \frac{4\Gamma_{jL}\Gamma_{jR}}{\Gamma_{jL} + \Gamma_{jR}} \int d\omega \pi A_{j\sigma}(\omega) \left(-\frac{\partial f(\omega)}{\partial \omega} \right), \quad (5)$$

where $f(\omega)$ denotes the Fermi-Dirac distribution function and $A_{j\sigma}(\omega)$ is the spectral function of quantum dot j for spin σ . The conductance through the dot j is then given by $G_j = \sum_{\sigma} G_{j\sigma}$, while the total conductance can be simply expressed as $G = \sum_j G_j$.

In the following we assume symmetric couplings, $\Gamma_{rj} = \Gamma/2$ and take $U_1 = U_2 \equiv U$. In NRG calculations we keep at least $N_K = 10000$ states during the iteration and use the band discretization parameter $\Lambda = 2-2.5$. Moreover, we make use of the spin and the charge conservation of the first dot coupled to its leads. We also exploit the conservation of spin-up particles and the charge parity for the second dot coupled to external leads and to the Majorana wire.

III. RESULTS AND DISCUSSION

In this section we present and discuss the numerical results on the transport properties of the considered double dot-Majorana setup. We start the considerations with the analysis of the spectral functions. Then, we study the gate voltage dependence of the linear conductance for different couplings to topological superconductor. Finally, we analyze the temperature dependence of the conductance. We generally focus on the case of a long topological superconducting wire, such that the overlap between the Majorana zero-energy modes is negligible $\varepsilon_M \rightarrow 0$. However, to make the discussion complete, we also analyze the transport behavior in the short nanowire case, when $\varepsilon_M \neq 0$.

The considered double dot system exhibits various transport regimes, where both $SU(4)$ as well as spin or orbital $SU(2)$ Kondo effects can develop [48, 49, 52, 53, 55, 57]. Given the large diversity of the parameter space, in this paper we focus on the case when the position of the energy level of each dot is the same, i.e. $\varepsilon_1 = \varepsilon_2 \equiv \varepsilon$. This condition can be obtained by an appropriate tuning of the gate voltages [57]. In a such case, in the absence of topological superconducting wire, the double dot

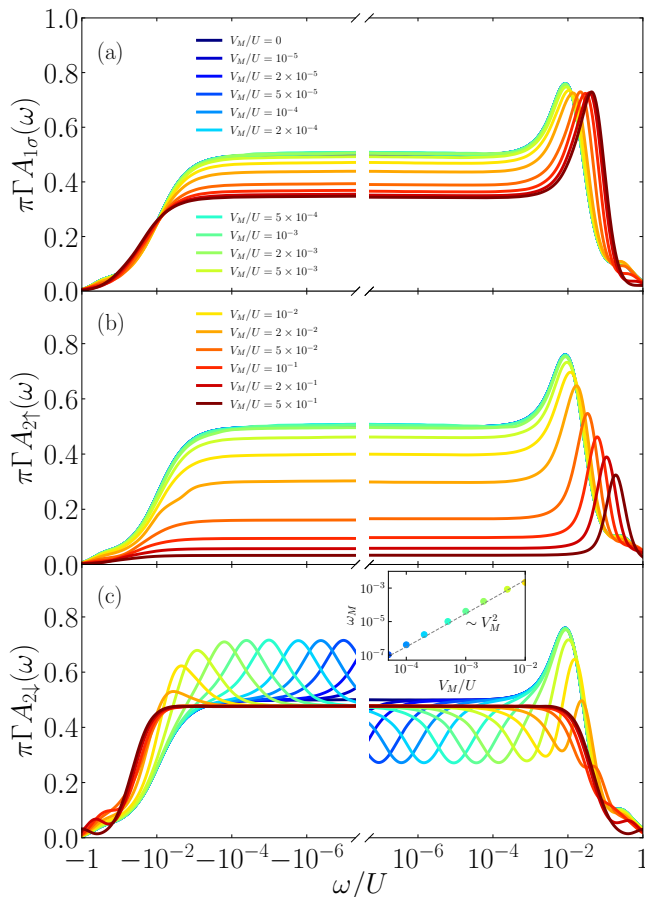


FIG. 2. The energy dependence of the normalized spectral function of (a) the first quantum dot, the second quantum dot for (b) spin-up and (c) spin-down calculated for different values of the coupling to the Majorana wire V_M , as indicated. The inset in (c) demonstrates the scaling of the position of local minima in $A_{2\downarrow}(\omega)$, denoted as ω_M , with the coupling V_M . The other parameters are: $U = 1$, $U' = 0.5$, $\Gamma = 0.05$, $\varepsilon_1 = \varepsilon_2 = -U'/2$, $T = 0$ and $\varepsilon_M = 0$ in units of band halfwidth.

should be empty for $\varepsilon \gtrsim 0$, singly occupied occupied when $-U' \lesssim \varepsilon \lesssim 0$, doubly occupied with one electron on each dot for $-U' - U \lesssim \varepsilon \lesssim -U'$, occupied by three electrons when $-2U' - U \lesssim \varepsilon \lesssim -U' - U$ and the occupation would be full once $\varepsilon \lesssim -2U' - U$. In the transport regime where the DQD occupation is odd, the system should exhibit the $SU(4)$ Kondo effect. On the other hand, in the case when the double dot is occupied with a single electron on each quantum dot the spin $SU(2)$ Kondo effect develops on every dot. Below, we thoroughly address the system's transport properties in these two regimes.

A. The spectral functions

1. The $SU(4)$ Kondo regime

Let us first discuss the behavior of the spectral functions of the double quantum dot system in the $SU(4)$ Kondo regime. This Kondo regime is realized when the double dot is occupied by a single electron and four-fold degeneracy due to the orbital and spin degrees of freedoms is present, which happens for $\varepsilon_1 = \varepsilon_2 = -U'/2$ [49, 57]. The corresponding spectral functions are presented in Fig. 2 for different values of the coupling to Majorana wire V_M . In the case of $V_M = 0$, one can recognize the Kondo resonance displaced from the Fermi level, a characteristic feature of the $SU(4)$ Kondo effect. Moreover, one then finds $A_{1\sigma}(0) = A_{2\sigma}(0) = 1/2\pi\Gamma$, which results in $G = \sum_{j\sigma} G_{j\sigma} = 2e^2/h$ [49, 57]. Increasing the coupling to Majorana zero-energy mode gives rise to a slight decrease of $A_{1\sigma}(0)$ and shift of the Kondo peak to larger energies, see Fig. 2(a).

On the other hand, more interesting behavior can be observed for the spectral function of the second dot, which is in a direct proximity with topological superconductor. In the case of spin-up component, one observes a decrease of $A_{2\uparrow}(0)$ once $V_M \gtrsim 0.005U \approx T_K^{SU(4)}$, see Fig. 2(b), where $T_K^{SU(4)}$ is the $SU(4)$ Kondo temperature, the magnitude of which can be estimated from the displacement of the spectral function peak from the Fermi level. However, now, contrary to the case of the first dot, the suppression of $A_{2\uparrow}(0)$ is much larger with increasing V_M . This behavior can be understood by realizing that the coupling to Majorana wire induces a spin splitting of the dot level, when the level position is detuned from the particle-hole symmetry point. Such splitting occurs in the second dot, and for a single dot proximized by Majorana wire, but decoupled from normal leads, it can be expressed as [39, 42]

$$\Delta\varepsilon_2 = \varepsilon_2 + \frac{U}{2} + \frac{1}{2}\sqrt{\varepsilon_2^2 + V_M^2} - \frac{1}{2}\sqrt{(\varepsilon_2 + U)^2 + V_M^2}.$$

In the case of $\varepsilon_2 = -U'/2$, by expanding in the leading order in V_M , one obtains

$$\Delta\varepsilon_2 \approx \frac{(U - U')V_M^2}{(2U - U')U'}. \quad (6)$$

Thus, when $\Delta\varepsilon_2 \gtrsim T_K^{SU(4)}$, $A_{2\uparrow}(\omega)$ starts depending on V_M and the position of the peak in the spectral function moves according to $\omega \approx \Delta\varepsilon_2 \sim V_M^2$.

Because the Majorana mode is assumed to be coupled to the spin-down level of the second dot, its influence is most pronounced in $A_{2\downarrow}(\omega)$. Now, however, one observes new features resulting from the quantum interference with Majorana mode when the coupling V_M is smaller than the Kondo energy scale. Interestingly, a local maximum (minimum) develops when $V_M \lesssim T_K^{SU(4)}$ at negative (positive) energies $|\omega| \equiv \omega_M$. The minimum

moves to larger energies with increasing V_M and generates an anti-resonance visible in $A_{2\downarrow}(\omega)$ for $\omega \approx T_K^{SU(4)}$, until it disappears once $V_M \gtrsim T_K^{SU(4)}$. On the other hand, the maximum visible for $\omega < 0$ moves to larger negative energies and fades out when the coupling V_M becomes greater than the Kondo temperature. When this happens, the spectral function exhibits just a broad plateau with $A_{2\downarrow}(0) = 1/2\pi\Gamma$, see Fig. 2(c). As presented in the inset of Fig. 2(c), the position of the local minimum and maximum depends on the coupling to topological wire as $\omega_M \sim V_M^2$.

The effect of finite overlap of Majorana zero-energy modes on the spectral functions is presented in Fig. 3. Because this influence is most visible in the case of the spin-down spectral function of the second dot, in the figure we present only this correlation function, while we note that the impact of ε_M on the other spectral functions is very weak and does not lead to qualitative changes for the considered values of ε_M . As known from the single quantum dot case [39, 42], the splitting of the Majorana zero-energy modes destroys the quantum interference and can give rise to the restoration of the Kondo resonance in the spectral function. A similar scenario can be observed in the case of double quantum dots in the spin-charge entangled regime, now, however, the dependence on ε_M is much more subtle. First of all, it can be seen that the energy scale associated with ε_M is clearly visible in the behavior of $A_{2\downarrow}(\omega)$. For positive (negative) energies the spectral function displays a minimum (maximum) for $|\omega| \lesssim T_K^{SU(4)}$ as long as this local extremum occurs for $|\omega| \gtrsim \varepsilon_M$, i.e. as long as $\omega_M \gtrsim \varepsilon_M$. On the other hand, for small energies, such that $|\omega| \lesssim \varepsilon_M$, a new local maximum (minimum) develops in $A_{2\downarrow}(\omega)$, see Figs. 3(a)-(c). This change in the behavior is observed when the overlap is smaller than the corresponding Kondo temperature, $\varepsilon_M \lesssim T_K^{SU(4)}$. For $\varepsilon_M \gtrsim T_K^{SU(4)}$, however, the local extrema are no longer visible, instead, a pronounced resonance develops at the Fermi energy for large enough coupling to Majorana wire, see Fig. 3(d). This resonance signals the orbital Kondo effect, since the spin-degeneracy is broken by the coupling to topological superconducting wire.

2. The $SU(2)$ Kondo regime

Now we focus on the transport regime where both quantum dots are singly occupied, such that, in the absence of coupling to Majorana wire, the spin $SU(2)$ Kondo effect can develop in each dot separately. The relevant spectral functions in the case of $\varepsilon_1 = \varepsilon_2 = -U/2 - U'$ calculated for different values of V_M are shown in Fig. 4. First of all, one can note that the spectral function of the first dot very weakly depends on V_M , while the main impact is revealed in the behavior of $A_{2\sigma}(\omega)$. This is quite natural since for $\varepsilon = -U/2 - U'$ each quantum dot forms the Kondo state with its own leads and the

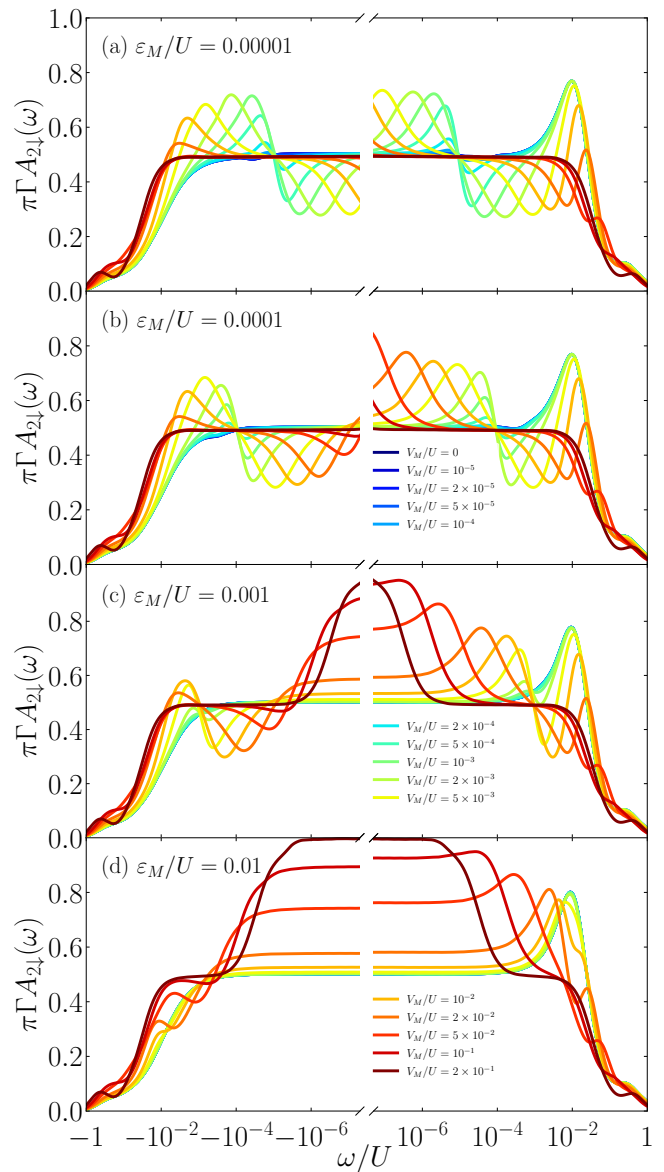


FIG. 3. The energy dependence of the spin-down spectral function of the second quantum dot for different values of the coupling to Majorana wire, as indicated, and for finite overlap between Majorana modes: (a) $\varepsilon_M/U = 0.00001$, (b) $\varepsilon_M/U = 0.0001$, (c) $\varepsilon_M/U = 0.001$ and (d) $\varepsilon_M/U = 0.01$. The other parameters are the same as in Fig. 2.

relevant energy scale for this state is given by intra-dot correlations and not inter-dot ones as was in the case of the $SU(4)$ Kondo effect. Consequently, the coupling to topological superconducting wire has the main effect on the second dot spectral function. Moreover, the dependence of $A_{2\sigma}(\omega)$ on V_M resembles now that predicted for the case of a single quantum dot coupled to Majorana wire [39, 42]. One can clearly recognize an energy scale associated with the coupling to Majorana wire, ω_M , which gives rise to a local maximum visible in the spin-down spectral function for low values of V_M , see Fig. 4(c).

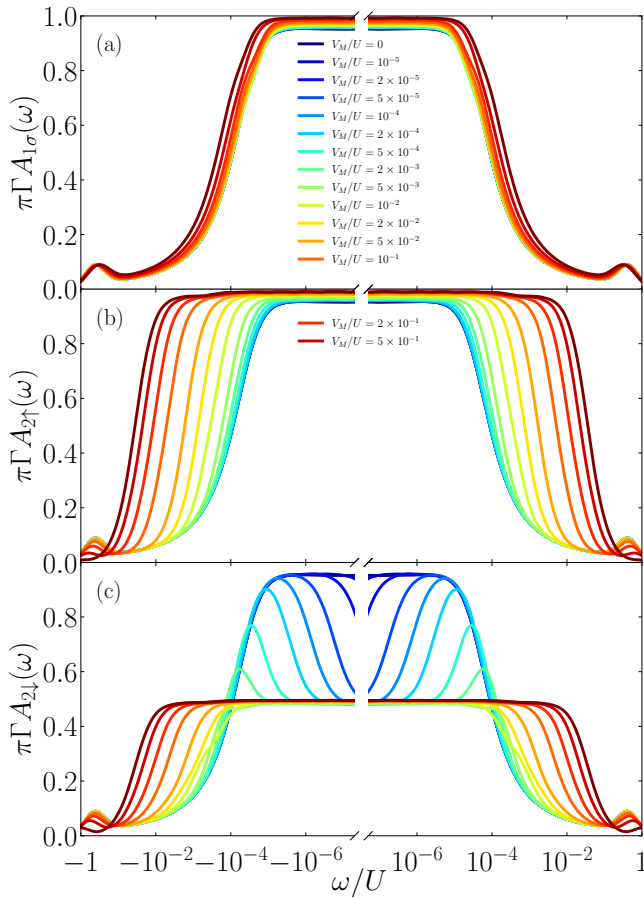


FIG. 4. The normalized spectral function of (a) the first quantum dot, the second quantum dot for (b) spin-up and (c) spin-down calculated for $\varepsilon_1 = \varepsilon_2 = -U/2 - U'$ and for different values of the coupling to the Majorana wire V_M , as indicated. The other parameters are the same as in Fig. 2.

Further enhancement of V_M , such that $V_M \gtrsim T_K^{SU(2)}$, results in the formation of a plateau at the Fermi energy of height $A_{2\downarrow}(0) = 1/2\pi\Gamma$, whose width grows with increasing V_M . This indicates an increase of the associated Kondo temperature, which can be related to the width of the spectral function resonance at the Fermi level, see Figs. 4(b) and (c). It is important to note that, while the coupling to Majorana wire modifies the Kondo temperature of second dot, $T_K^{SU(2)}$ of the first dot hardly depends on V_M . Consequently, although the double dot may still be in the $SU(2)$ Kondo regime, the strength of Kondo correlations on each dot can be different.

We also analyze the effect of finite length of the Majorana wire on the spectral functions in the corresponding transport regime. As $A_{1\sigma}(\omega)$ hardly depends on V_M , it is also independent of ε_M . The dependence of the spin-up spectral function of the second dot on ε_M is mainly quantitative, while no qualitative changes are observed—finite ε_M slightly affects the width of the Kondo resonance, while its height is not affected. Therefore, in Fig. 5 we only present the dependence of $A_{2\downarrow}(\omega)$ on the over-

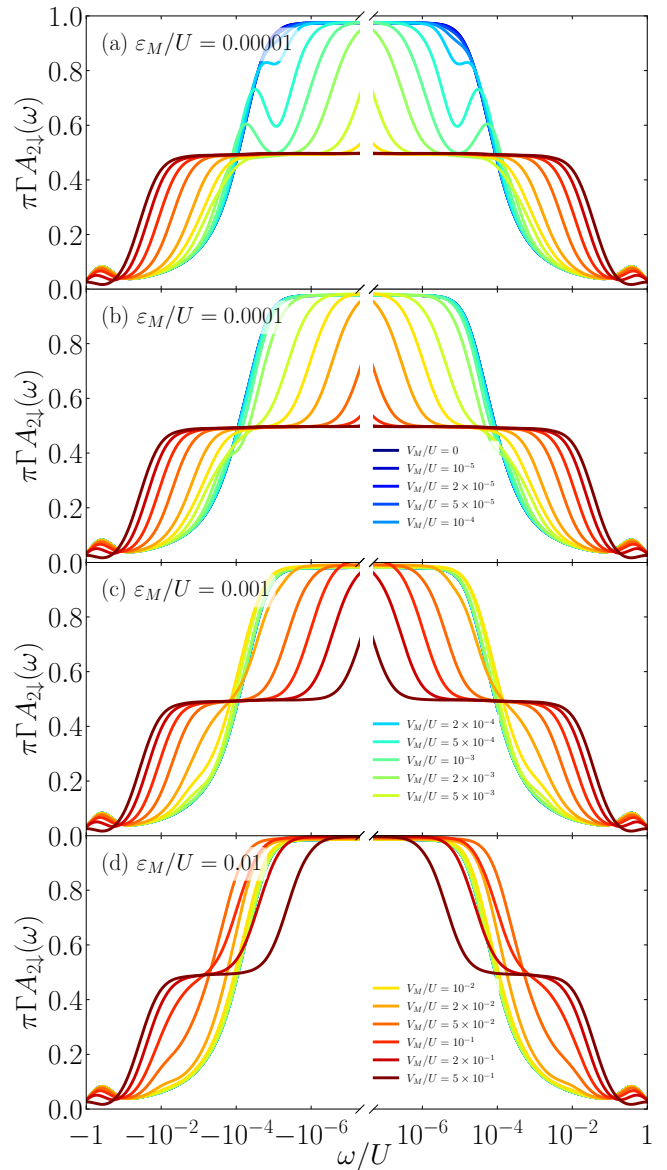


FIG. 5. The normalized spin-down spectral function of the second dot calculated for (a) $\varepsilon_M/U = 0.00001$, (b) $\varepsilon_M/U = 0.0001$, (c) $\varepsilon_M/U = 0.001$ and (d) $\varepsilon_M/U = 0.01$ for different values of the coupling to the Majorana wire V_M , as indicated. The other parameters are the same as in Fig. 4.

lap of Majorana quasiparticles. When comparing with Fig. 4(c), one can see that finite ε_M suppresses the quantum interference with the Majorana wire and the local maximum visible in $A_{2\downarrow}(\omega)$ for $V_M = 0$ at low energies becomes diminished. Moreover, larger values of ε_M give rise to the restoration of the Kondo peak in the spectral function. A similar behavior has been observed in the case of single quantum dots [39, 42].

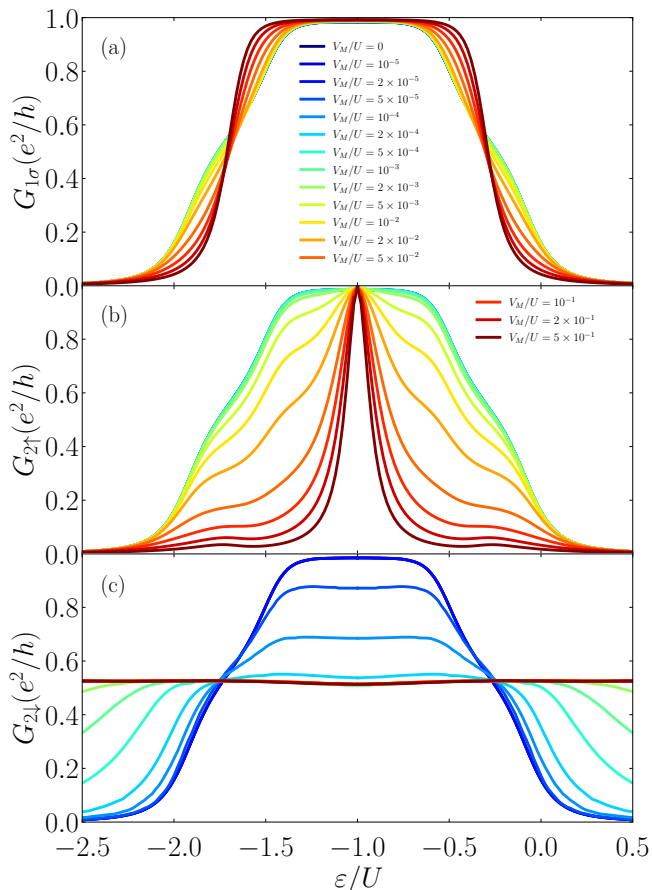


FIG. 6. The double dot level dependence of the spin-resolved linear conductance of (a) the first quantum dot $G_{1\sigma}$, (b) the spin-up $G_{2\uparrow}$ and (c) spin-down $G_{2\downarrow}$ conductance of the second dot. The conductance is plotted vs. $\epsilon_1 = \epsilon_2 \equiv \epsilon$ and calculated for different values of the coupling to the Majorana wire, as indicated. The other parameters are the same as in Fig. 2 with $T/U = 5 \cdot 10^{-7}$.

B. Gate voltage dependence of conductance

The spin-resolved linear conductance of both quantum dots as a function of the double dot energy levels $\epsilon_1 = \epsilon_2 \equiv \epsilon$ and calculated for different values of coupling to Majorana wire is shown in Fig. 6. This figure has been calculated at temperature $T/U = 5 \cdot 10^{-7}$, which is smaller than the characteristic Kondo scales in the system. Since the position of the quantum dot levels can be changed by gate voltages applied to the dots [57], this figure effectively presents the gate voltage dependence of the conductance.

When $V_M = 0$ all conductances are equal and one observes the evolution of $G_{j\sigma}$ with the level position, which is typical for correlated double dots [57]. For $\epsilon \gtrsim 0$, transport is dominated by elastic cotunneling and the conductance is low. Then, with lowering ϵ , one enters the $SU(4)$ Kondo regime and $G_{j\sigma} = e^2/2h$ for $\epsilon = -U'/2$. When both dots become singly occupied, which happens when

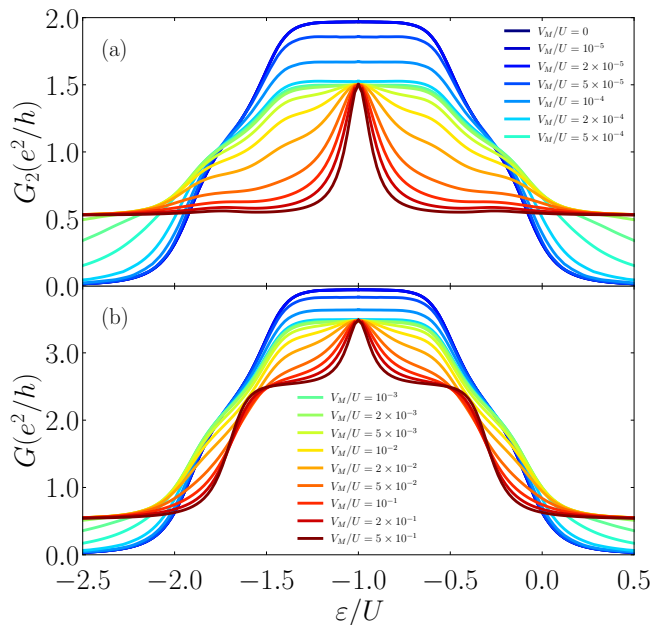


FIG. 7. The linear conductance of (a) the second dot G_2 and (b) the total conductance G calculated as a function of $\epsilon_1 = \epsilon_2 \equiv \epsilon$ for different values of the coupling to the Majorana wire. The parameters are the same as in Fig. 6.

$\epsilon \lesssim -U'$, the conductance is given by $G_{j\sigma} = e^2/h$ due to the spin $SU(2)$ Kondo effect in each dot. Note that all the curves are symmetric with respect to the particle-hole symmetry point of the double dot system, $\epsilon = -U/2 - U'$, see Fig. 6.

When the coupling to Majorana wire is turned on, the level dependence of conductance becomes modified. This modification is the largest in the case of the second dot, while $G_{1\sigma}$ only weakly depends on V_M , cf. Fig. 6(a) with Figs. 6(b) and (c). In particular, the value of $G_{1\sigma} = e^2/h$ around the particle-hole symmetry point hardly depends on V_M , while the width of this plateau increases with V_M . In fact, the largest changes of $G_{1\sigma}$ can be observed in the $SU(4)$ Kondo regime around $\epsilon = -U'/2$, see Fig. 6(a). This is just contrary to the behavior of conductance through the second dot, which strongly depends on the strength of coupling to topological wire in the full range of ϵ , see Figs. 6(b) and (c), except for the particle-hole symmetry point of the double dot, $\epsilon = -U/2 - U'$, in the case of $G_{2\uparrow}$, where the value of $G_{2\uparrow}$ stays intact as V_M is varied. Generally, the coupling V_M generates a spin-splitting of the second dot level, which inevitably affects the Kondo state. For the spin-up conductance component, this results in the suppression of $G_{2\uparrow}$ except for the particle hole-symmetry point. On the other hand, for the spin-down component we observe a mixed behavior: in the $SU(2)$ Kondo regime the conductance becomes decreased, while in other regimes it increases with V_M until the conductance eventually reaches $G_{2\downarrow} \approx e^2/2h$, irrespective of ϵ , once V_M is larger than the corresponding Kondo scales, see Fig. 6(c). Interestingly, one can also see

that with increasing V_M $G_{2\sigma}$ first starts changing in the $SU(2)$ Kondo regime as compared to the $SU(4)$ Kondo regime. This is due to the fact that $T_K^{SU(2)} < T_K^{SU(4)}$, thus, a smaller value of coupling to Majorana wire is necessary to affect the conductance in the spin Kondo regime. It is also important to note that for $\varepsilon/U \approx -0.25$ and $\varepsilon/U \approx -1.25$, the conductance $G_{2\downarrow}$ has a stable point in some range of V_M , see Fig. 6(c). This is in fact the middle of the $SU(4)$ Kondo regime where, because of that, the conductance becomes affected by V_M only when the coupling to Majorana wire is larger than the corresponding Kondo temperature.

Figure 7 presents the full conductance through the second dot, $G_2 = \sum_{\sigma} G_{2\sigma}$, as well as the total conductance through the system G . Now, one can clearly recognize the influence of the presence of topological superconductor hosting Majorana quasiparticles on the transport behavior of strongly-correlated DQD. Finite coupling V_M results in fractional values of G_2 , namely, $G_2 = 3e^2/2h$ for $\varepsilon \approx -U/2 - U'$, while $G_2 = e^2/2h$ otherwise. In consequence, the total conductance in the $SU(2)$ Kondo regime is given by $G = 5e^2/2h$ except for $\varepsilon \approx -U/2 - U'$, where it reaches $G = 7e^2/2h$. Note that if the coupling to Majorana wire is not large, $V_M/U \lesssim 10^{-3}$, $G = 7e^2/2h$ in the $SU(2)$ Kondo regime. On the other hand, for $\varepsilon \gtrsim 0$ ($\varepsilon \lesssim -U - 2U'$) it becomes $G = e^2/2h$. These fractional values are clear signatures of the presence of Majorana zero-energy modes in the system.

The effect of finite overlap between the Majorana quasiparticles on the gate voltage dependence of the linear conductance is presented in Fig. 8. Because for assumed parameters the impact on both G_1 and $G_{2\uparrow}$ is rather weak, we only present the spin-down component of the conductance through the second dot, together with G_2 and G , in which the impact of ε_M becomes visible. Comparing Fig. 8(a) with Fig. 6(c), one can see that the change in the behavior is considerable. This is related to the fact that the splitting of Majorana zero-energy modes suppresses the quantum interference with the topological superconductor. One can see that when $\varepsilon_M > 0$, increasing the coupling to the Majorana wire results in an overall suppression of $G_{2\downarrow}$ in the two-electron transport regime, i.e. for $-U - U' \lesssim \varepsilon \lesssim -U'$, except for the particle-hole symmetry point $\varepsilon = -U/2 - U'$. In this transport regime each of the dots exhibits the $SU(2)$ Kondo effect and the behavior of $G_{2\downarrow}$ is in fact consistent with what has been observed in the case of single quantum dots coupled to Majorana wire [42]. The coupling to topological superconductor results in a spin splitting of the dot level, which is somewhat similar to the exchange field induced in the case of quantum dots attached to ferromagnetic leads [67]. This gives rise to the suppression of the conductance except for the particle-hole symmetry point. In the transport regime where the double dot is either empty or fully occupied, one can see that finite ε_M is responsible for the suppression of the conductance; $G_{2\downarrow}$ does not saturate at $e^2/2h$ with increasing V_M any more, instead it becomes suppressed. The above described be-

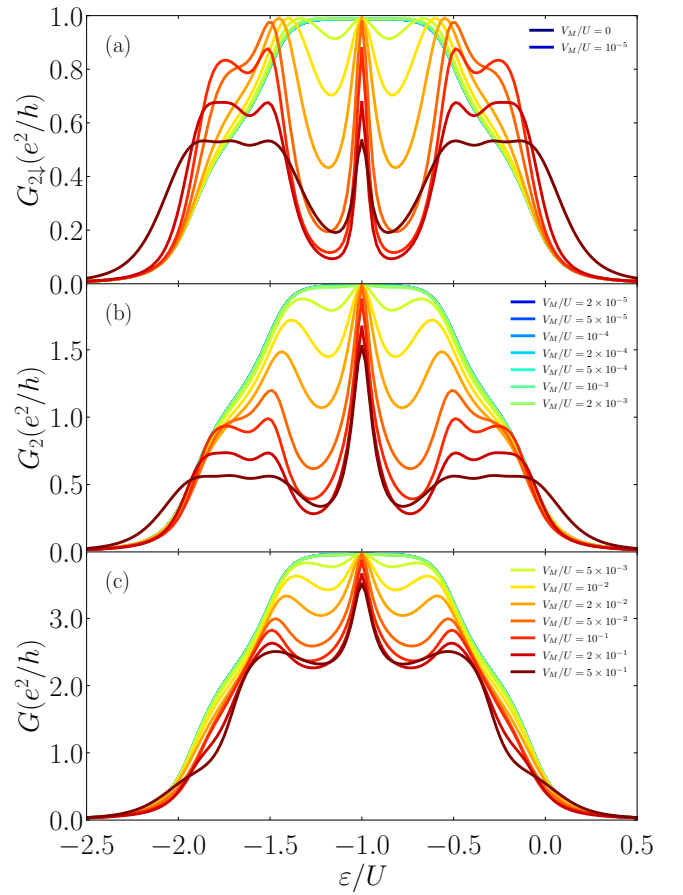


FIG. 8. The gate voltage dependence of (a) the spin-down linear conductance of the second dot, (b) the full conductance through the second dot as well as (c) the total conductance through the system G . The conductance is plotted vs. $\varepsilon_1 = \varepsilon_2 \equiv \varepsilon$ and calculated for different values of the coupling to the Majorana wire, as indicated, and for finite overlap between Majorana quasiparticles $\varepsilon_M/U = 0.001$. The other parameters are the same as in Fig. 6.

havior is revealed in the behavior of the total conductance through the second dot [Fig. 8(b)] and the total conductance through the system [Fig. 8(c)]. The main observation is that finite overlap of Majorana modes changes the fractional values of the conductance present in the case of $\varepsilon_M = 0$. The conductance plateau in the middle of the gate voltage dependence is destroyed and, instead, only a peak with $G_2 = 2e^2/h$ ($G = 4e^2/h$) for $\varepsilon = -U/2 = U'$ is present. On the other hand, for $\varepsilon \gtrsim 0$ ($\varepsilon \lesssim -U - 2U'$), both G_2 and G are generally suppressed.

C. Temperature dependence of conductance

In this section we present and discuss the effect of coupling to Majorana wire on the temperature dependence of linear conductance. We first focus on the case when the system exhibits the $SU(4)$ Kondo effect in the ab-

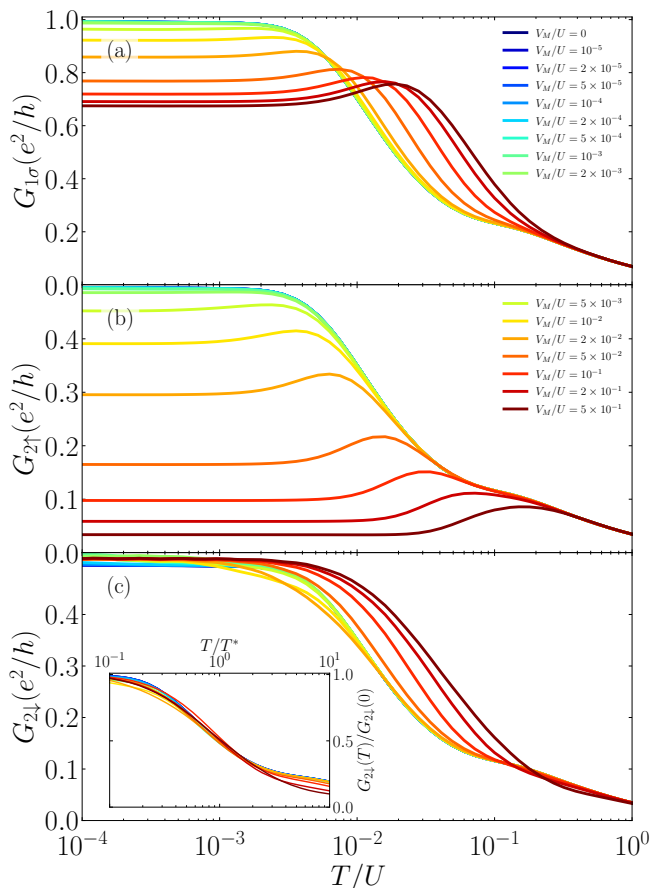


FIG. 9. The temperature dependence of the linear conductance of (a) the first quantum dot, the second quantum dot for (b) spin-up and (c) spin-down calculated for $\varepsilon_1 = \varepsilon_2 = -U'/2$ and different values of the coupling to the Majorana wire, as indicated. The inset in (c) presents the normalized conductance $G_{2\downarrow}(T)/G_{2\downarrow}(0)$ as a function of T/T^* , where T^* is the temperature at which $G_{2\downarrow}(T)/G_{2\downarrow}(0) = 1/2$. The other parameters are the same as in Fig. 2.

sence of Majorana wire and then proceed to the case of the spin $SU(2)$ Kondo regime.

1. The $SU(4)$ Kondo regime

The quantum dot- and spin-resolved conductance as a function of temperature calculated for $\varepsilon_1 = \varepsilon_2 = -U'/2$ is displayed in Fig. 9. For $V_M = 0$, the conductance displays a scaling behavior characteristic of the $SU(4)$ Kondo regime. When the coupling to the Majorana wire is turned on, with its grow, one observes a gradual distortion of the universal conductance curve. When V_M is sufficiently large, G_1 exhibits a small drop of its low-temperature value, while a local maximum develops around $T \approx T_K^{SU(4)}$, which moves to higher temperatures with increasing V_M , see Fig. 9(a). Much larger influence is visible in the case of the second dot, where almost

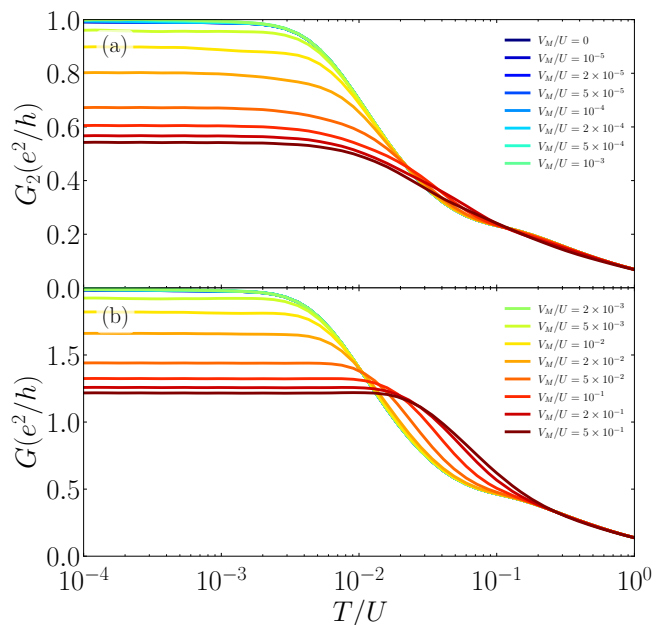


FIG. 10. The temperature dependence of the linear conductance of (a) the second quantum dot, (b) and the total conductance of the system, calculated for different values of the coupling to the Majorana wire. The parameters are the same as in Fig. 9.

a full suppression of the conductance is visible in the spin-up channel, with a local maximum at the temperatures corresponding to a similar behavior present in G_1 [Fig. 9(b)]. On the other hand, the spin-down channel of the second dot reveals a weaker dependence on V_M . The low-temperature maximum of $G_{2\downarrow}$ basically does not depend on V_M , whereas the temperature at which the conductance reaches maximum slightly increases with V_M . In the inset of Fig. 9(c) we present explicitly the scaling behavior of the conductance $G_{2\downarrow}$. The normalized conductance $G_{2\downarrow}(T)/G_{2\downarrow}(0)$ is plotted vs T/T^* , where T^* is the temperature at which the conductance drops to a half of its low-temperature value. Consequently, for V_M , one has $T^* = T_K^{SU(4)}$, which yields $T_K^{SU(4)}/U \approx 0.019$. One can see that for finite V_M the temperature dependence of the normalized conductance becomes modified and it deviates from the $SU(4)$ scaling.

The conductance through the second dot and the total conductance of the system as a function of temperature are shown in Fig. 10. One can now clearly see that increasing V_M results in lowering of the low-temperature conductance. Moreover, a slight increase of the temperature at which the conductance starts raising due to the Kondo effect is also visible.

2. The $SU(2)$ Kondo regime

Figure 11 presents the temperature dependence of the spin-resolved conductance through each dot calculated

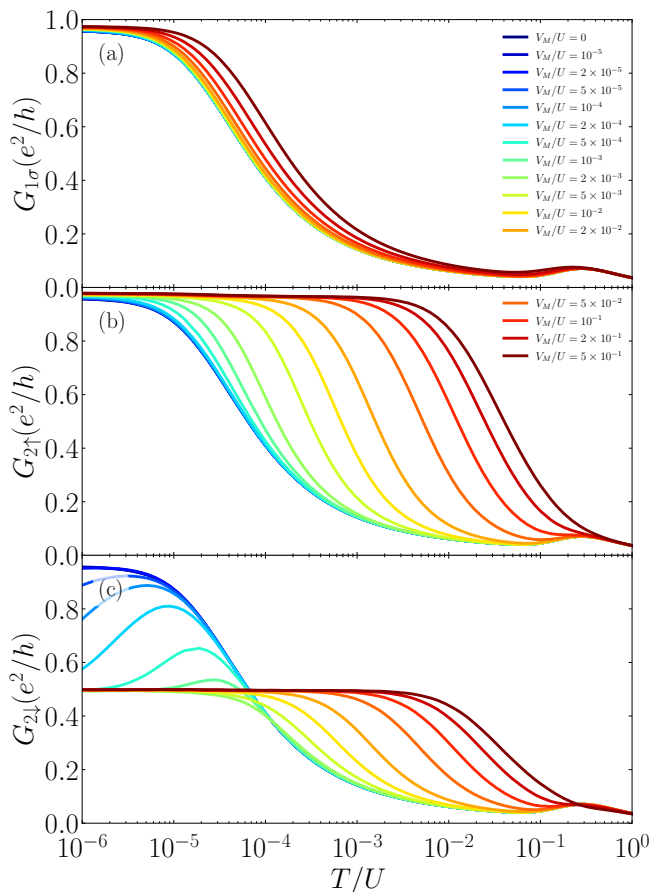


FIG. 11. The temperature dependence of the linear conductance of (a) first quantum dot, the second quantum dot for (b) spin-up and (c) spin-down calculated for $\varepsilon_1 = \varepsilon_2 = -U/2 - U'$ and for different values of the coupling to the Majorana wire, as indicated. The other parameters are the same as in Fig. 4.

for different temperatures and assuming $\varepsilon = -U/2 - U'$. When $V_M = 0$, the system exhibits the Kondo effect on every quantum dot and the conductance reaches its maximum value, i.e. $G_{j\sigma} = e^2/h$. When the coupling to Majorana wire is turned on, it very weakly affects the temperature dependence of $G_{1\sigma}$, while the largest changes can be seen in the behavior of $G_{2\sigma}$. More specifically, in the case of the first dot one only observes a small increase of the corresponding Kondo temperature. This is contrary to $G_{2\uparrow}$, which exhibits a strong enhancement of the Kondo temperature with increasing V_M , see Fig. 11(b). A similar enhancement of energy scale at which conductance increases can be observed in the case of $G_{2\downarrow}$ shown in Fig. 11(c). Now, however, one can see a nonmonotonic behavior of conductance for small values of V_M and consecutive suppression of the low-temperature conductance to $G_{2\downarrow} = e^2/2h$.

To make the picture complete, in Fig. 12 we show the total conductance through the second dot and the total conductance through the system. The temperature dependence of G_2 shows a characteristic dip at low tem-

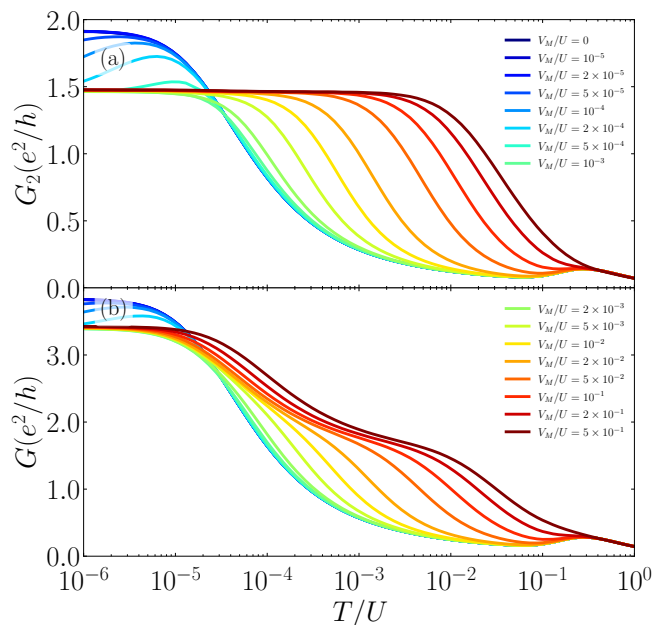


FIG. 12. The temperature dependence of (a) the total conductance through the second dot and (b) the total conductance through the system for different values of V_M . The parameters are the same as in Fig. 11.

peratures and low values of V_M , resulting from the quantum interference with the Majorana wire. This behavior bears some resemblance to the single quantum dot case [42]. On the other hand, the total conductance for larger values of coupling to topological superconductor exhibits a two-step increase with lowering the temperature. First, G reaches the value of the order of $3e^2/2h$ and then, with further decrease of T , it approaches $G = 7e^2/2h$, see Fig. 12(b).

IV. CONCLUSIONS

We have analyzed the transport properties of strongly correlated double quantum dot coupled to the Majorana wire. The calculations have been performed with the aid of the numerical renormalization group method. The main focus was on the signatures and impact of Majorana quasiparticles on spin-charge entangled Kondo regime of the system. However, we have also addressed the transport regime where the system exhibits the spin Kondo effect. In particular, we have comprehensively analyzed the spectral functions of the dots as well as the gate voltage and temperature dependence of the linear conductance. We have considered the case of a long Majorana wire, however, the effect of finite overlap of Majorana zero-energy modes has also been addressed.

We have shown that in the $SU(4)$ Kondo regime the spectral function of the dot in the vicinity of topological superconductor exhibits a local minimum (maximum) on either side of the Fermi level. Moreover, in the case of fi-

nite overlap between Majorana modes, a local maximum and minimum may occur both for positive and negative energies, indicating the energy scale associated with the splitting of Majorana quasiparticles. In the Coulomb valley with a single electron on each dot, the coupling to Majorana wire results in a local minimum at low energies visible in the spin-down spectral function of the second dot. This feature becomes however suppressed when the Majorana wire is relatively short.

The behavior of the spectral functions is directly revealed in the linear conductance. Studying the gate voltage dependence of spin-resolved conductance, we have identified transport regimes where G reaches fractional values, which stem from the presence of Majorana quasiparticles in the system. We have also demonstrated that these fractional conductance features may become suppressed if a considerable overlap between Majorana modes is present. Finally, we have determined the temperature dependence of the conductance shedding light on its behavior both in the spin-charge entangled regime

as well as in the transport regime where the system exhibits the spin $SU(2)$ Kondo effect. Deviations from universal scaling characteristic of those regimes are uncovered.

We believe that our study extends the knowledge on the interplay of Kondo correlations with topological superconducting wires hosting Majorana modes, fostering further efforts to study and understand the physics of two fundamental research areas: topological properties of matter and nontrivial Kondo states.

ACKNOWLEDGMENTS

This work was supported by the National Science Centre in Poland through the Project No. 2018/29/B/ST3/00937. The computing time at the Poznań Supercomputing and Networking Center is acknowledged.

-
- [1] A. Y. Kitaev, Unpaired Majorana fermions in quantum wires, *Phys. Usp.* **44**, 131 (2001).
- [2] R. M. Lutchyn, J. D. Sau, and S. Das Sarma, Majorana Fermions and a Topological Phase Transition in Semiconductor-Superconductor Heterostructures, *Phys. Rev. Lett.* **105**, 077001 (2010).
- [3] Y. Oreg, G. Refael, and F. von Oppen, Helical Liquids and Majorana Bound States in Quantum Wires, *Phys. Rev. Lett.* **105**, 177002 (2010).
- [4] J. Alicea, New directions in the pursuit of Majorana fermions in solid state systems, *Rep. Prog. Phys.* **75**, 076501 (2012).
- [5] H. Kim, A. Palacio-Morales, T. Posske, L. Rózsa, K. Palotás, L. Szunyogh, M. Thorwart, and R. Wiesendanger, Toward tailoring Majorana bound states in artificially constructed magnetic atom chains on elemental superconductors, *Sci. Adv.* **4**, eaar5251 (2018).
- [6] E. Prada, P. San-Jose, M. W. A. de Moor, A. Geresdi, E. J. H. Lee, J. Klinovaja, D. Loss, J. Nygård, R. Aguado, and L. P. Kouwenhoven, From Andreev to Majorana bound states in hybrid superconductor-semiconductor nanowires, *Nat. Rev. Phys.* **2**, 575 (2020).
- [7] V. Mourik, K. Zuo, S. M. Frolov, S. R. Plissard, E. P. A. M. Bakkers, and L. P. Kouwenhoven, Signatures of Majorana Fermions in Hybrid Superconductor-Semiconductor Nanowire Devices, *Science* **336**, 1003 (2012).
- [8] A. Das, Y. Ronen, Y. Most, Y. Oreg, M. Heiblum, and H. Shtrikman, Zero-bias peaks and splitting in an Al-InAs nanowire topological superconductor as a signature of Majorana fermions, *Nat. Phys.* **8**, 887 (2012).
- [9] M. T. Deng, C. L. Yu, G. Y. Huang, M. Larsson, P. Caroff, and H. Q. Xu, Anomalous Zero-Bias Conductance Peak in a Nb-InSb Nanowire-Nb Hybrid Device, *Nano Lett.* **12**, 6414 (2012).
- [10] H. O. H. Churchill, V. Fatemi, K. Grove-Rasmussen, M. T. Deng, P. Caroff, H. Q. Xu, and C. M. Marcus, Superconductor-nanowire devices from tunneling to the multichannel regime: Zero-bias oscillations and magnetoconductance crossover, *Phys. Rev. B* **87**, 241401(R) (2013).
- [11] A. D. K. Finck, D. J. Van Harlingen, P. K. Mohseni, K. Jung, and X. Li, Anomalous Modulation of a Zero-Bias Peak in a Hybrid Nanowire-Superconductor Device, *Phys. Rev. Lett.* **110**, 126406 (2013).
- [12] S. M. Albrecht, A. P. Higginbotham, M. Madsen, F. Kuemmeth, T. S. Jespersen, J. Nygård, P. Krogstrup, and C. M. Marcus, Exponential protection of zero modes in Majorana islands, *Nature* **531**, 206 (2016).
- [13] M. T. Deng, S. Vaitiekėnas, E. B. Hansen, J. Danon, M. Leijnse, K. Flensberg, J. Nygård, P. Krogstrup, and C. M. Marcus, Majorana bound state in a coupled quantum-dot hybrid-nanowire system, *Science* **354**, 1557 (2016).
- [14] S. Jeon, Y. Xie, J. Li, Z. Wang, B. A. Bernevig, and A. Yazdani, Distinguishing a Majorana zero mode using spin-resolved measurements, *Science* **358**, 772 (2017).
- [15] F. Nichele, A. C. C. Drachmann, A. M. Whiticar, E. C. T. O'Farrell, H. J. Suominen, A. Fornieri, T. Wang, G. C. Gardner, C. Thomas, A. T. Hatke, P. Krogstrup, M. J. Manfra, K. Flensberg, and C. M. Marcus, Scaling of Majorana Zero-Bias Conductance Peaks, *Physical Review Letters* **119**, 136803 (2017), arXiv:1706.07033.
- [16] M.-T. Deng, S. Vaitiekėnas, E. Prada, P. San-Jose, J. Nygård, P. Krogstrup, R. Aguado, and C. M. Marcus, Nonlocality of Majorana modes in hybrid nanowires, *Phys. Rev. B* **98**, 085125 (2018).
- [17] R. M. Lutchyn, E. P. A. M. Bakkers, L. P. Kouwenhoven, P. Krogstrup, C. M. Marcus, and Y. Oreg, Majorana zero modes in superconductor-semiconductor heterostructures, *Nat. Rev. Mater.* **3**, 52 (2018).
- [18] Ö. Gül, H. Zhang, J. D. S. Bommer, M. W. A. de Moor, D. Car, S. R. Plissard, E. P. A. M. Bakkers, A. Geresdi, K. Watanabe, T. Taniguchi, and L. P. Kouwenhoven, Ballistic Majorana nanowire devices, *Nat. Nanotechnol.* **13**, 192 (2018).

- [19] H. Zhang, D. E. Liu, M. Wimmer, and L. P. Kouwenhoven, Next steps of quantum transport in Majorana nanowire devices, *Nature Communications* **10**, 5128 (2019).
- [20] A. Y. Kitaev, Fault-tolerant quantum computation by anyons, *Ann. Phys.* **303**, 2 (2003), publisher: Academic Press.
- [21] C. Nayak, S. H. Simon, A. Stern, M. Freedman, and S. Das Sarma, Non-Abelian anyons and topological quantum computation, *Rev. Mod. Phys.* **80**, 1083 (2008).
- [22] J. Alicea, Y. Oreg, G. Refael, F. von Oppen, and M. P. A. Fisher, Non-Abelian statistics and topological quantum information processing in 1D wire networks, *Nature Physics* **7**, 412 (2011).
- [23] D. E. Liu and H. U. Baranger, Detecting a Majorana-fermion zero mode using a quantum dot, *Phys. Rev. B* **84**, 201308(R) (2011).
- [24] M. Leijnse and K. Flensberg, Scheme to measure Majorana fermion lifetimes using a quantum dot, *Phys. Rev. B* **84**, 140501(R) (2011).
- [25] Y. Cao, P. Wang, G. Xiong, M. Gong, and X.-Q. Li, Probing the existence and dynamics of Majorana fermion via transport through a quantum dot, *Phys. Rev. B* **86**, 115311 (2012).
- [26] W.-J. Gong, S.-F. Zhang, Z.-C. Li, G. Yi, and Y.-S. Zheng, Detection of a Majorana fermion zero mode by a T-shaped quantum-dot structure, *Phys. Rev. B* **89**, 245413 (2014).
- [27] M. Cheng, M. Becker, B. Bauer, and R. M. Lutchyn, Interplay between Kondo and Majorana Interactions in Quantum Dots, *Phys. Rev. X* **4**, 031051 (2014).
- [28] D. E. Liu, M. Cheng, and R. M. Lutchyn, Probing Majorana physics in quantum-dot shot-noise experiments, *Phys. Rev. B* **91**, 081405(R) (2015).
- [29] A. Schuray, L. Weithofer, and P. Recher, Fano Resonances in Majorana Bound States - Quantum Dot Hybrid Systems, *Physical Review B* **96**, 085417 (2017), arXiv:1702.03909.
- [30] E. Prada, R. Aguado, and P. San-Jose, Measuring Majorana nonlocality and spin structure with a quantum dot, *Physical Review B* **96**, 085418 (2017).
- [31] S. Hoffman, D. Chevallier, D. Loss, and J. Klinovaja, Spin-dependent coupling between quantum dots and topological quantum wires, *Phys. Rev. B* **96**, 045440 (2017).
- [32] G. Górski, J. Barański, I. Weymann, and T. Domański, Interplay between correlations and Majorana mode in proximitized quantum dot, *Scientific Reports* **8**, 15717 (2018).
- [33] J. E. Sanches, L. S. Ricco, W. N. Mizobata, Y. Marques, M. de Souza, I. A. Shelykh, and A. C. Seridonio, Majorana molecules and their spectral fingerprints, *Physical Review B* **102**, 075128 (2020), arXiv:2004.00374.
- [34] K. Wrześniewski and I. Weymann, Magnetization dynamics in a Majorana-wire-quantum-dot setup, *Physical Review B* **103**, 125413 (2021).
- [35] E. Vernek, P. H. Penteado, A. C. Seridonio, and J. C. Egues, Subtle leakage of a Majorana mode into a quantum dot, *Phys. Rev. B* **89**, 165314 (2014).
- [36] D. A. Ruiz-Tijerina, E. Vernek, L. G. G. V. Dias da Silva, and J. C. Egues, Interaction effects on a Majorana zero mode leaking into a quantum dot, *Phys. Rev. B* **91**, 115435 (2015).
- [37] C.-X. Liu, J. D. Sau, T. D. Stanescu, and S. Das Sarma, Andreev bound states versus Majorana bound states in quantum dot-nanowire-superconductor hybrid structures: Trivial versus topological zero-bias conductance peaks, *Physical Review B* **96**, 075161 (2017).
- [38] T. Zienkiewicz, J. Barański, G. Górski, and T. Domański, Leakage of Majorana mode into correlated quantum dot nearby its singlet-doublet crossover, *J. Phys.: Condens. Matter* **32**, 025302 (2019).
- [39] M. Lee, J. S. Lim, and R. López, Kondo effect in a quantum dot side-coupled to a topological superconductor, *Phys. Rev. B* **87**, 241402(R) (2013).
- [40] A. Golub, I. Kuzmenko, and Y. Avishai, Kondo Correlations and Majorana Bound States in a Metal to Quantum-Dot to Topological-Superconductor Junction, *Phys. Rev. Lett.* **107**, 176802 (2011).
- [41] E. Eriksson, A. Nava, C. Mora, and R. Egger, Tunneling spectroscopy of Majorana-Kondo devices, *Physical Review B* **90**, 245417 (2014).
- [42] I. Weymann and K. P. Wójcik, Transport properties of a hybrid Majorana wire-quantum dot system with ferromagnetic contacts, *Phys. Rev. B* **95**, 155427 (2017).
- [43] I. Weymann, Spin Seebeck effect in quantum dot side-coupled to topological superconductor, *J. Phys.: Condens. Matter* **29**, 095301 (2017).
- [44] J. F. Silva, L. G. G. V. D. da Silva, and E. Vernek, Robustness of the Kondo effect in a quantum dot coupled to Majorana zero modes, *Phys. Rev. B* **101**, 075428 (2020).
- [45] I. Weymann, K. P. Wójcik, and P. Majek, Majorana-kondo interplay in t-shaped double quantum dots, *Phys. Rev. B* **101**, 235404.
- [46] J. F. Silva, L. G. G. V. D. da Silva, and E. Vernek, Robustness of the Kondo effect in a quantum dot coupled to Majorana zero modes, *Physical Review B* **101**, 075428 (2020).
- [47] A. C. Hewson, *The Kondo Problem to Heavy Fermions*, Cambridge Studies in Magnetism (Cambridge University Press, 1993).
- [48] M. Vojta, R. Bulla, and W. Hofstetter, Quantum phase transitions in models of coupled magnetic impurities, *Phys. Rev. B* **65**, 140405 (2002).
- [49] L. Borda, G. Zarand, W. Hofstetter, B. I. Halperin, and J. von Delft, $Su(4)$ fermi liquid state and spin filtering in a double quantum dot system, *Phys. Rev. Lett.* **90**, 026602 (2003).
- [50] N. J. Craig, J. M. Taylor, E. A. Lester, C. M. Marcus, M. P. Hanson, and A. C. Gossard, Tunable nonlocal spin control in a coupled-quantum dot system, *Science* **304**, 565 (2004).
- [51] T. Sato and M. Eto, Numerical renormalization group studies of $su(4)$ kondo effect in quantum dots, *Physica E: Low-Dimensional Systems and Nanostructures* **29**, 652 (2005).
- [52] M. R. Galpin, D. E. Logan, and H. R. Krishnamurthy, Quantum phase transition in capacitively coupled double quantum dots, *Phys. Rev. Lett.* **94**, 186406 (2005).
- [53] D. A. Ruiz-Tijerina, E. Vernek, and S. E. Ulloa, Capacitive interactions and kondo effect tuning in double quantum impurity systems, *Phys. Rev. B* **90**, 035119 (2014).
- [54] Y. Nishikawa, O. J. Curtin, A. C. Hewson, D. J. G. Crow, and J. Bauer, Conditions for observing emergent $su(4)$ symmetry in a double quantum dot, *Phys. Rev. B* **93**, 235115 (2016).
- [55] V. Lopes, R. A. Padilla, G. B. Martins, and E. V. Anda, $SU(4)$ - $SU(2)$ crossover and spin-filter properties of a dou-

- ble quantum dot nanosystem, *Phys. Rev. B* **95**, 245133 (2017).
- [56] S. Amasha, A. J. Keller, I. G. Rau, A. Carmi, J. A. Katine, H. Shtrikman, Y. Oreg, and D. Goldhaber-Gordon, Pseudospin-resolved transport spectroscopy of the kondo effect in a double quantum dot, *Phys. Rev. Lett.* **110**, 046604 (2013).
- [57] A. J. Keller, S. Amasha, I. Weymann, C. P. Moca, I. G. Rau, J. A. Katine, H. Shtrikman, G. Zaránd, and D. Goldhaber-Gordon, Emergent SU(4) Kondo physics in a spin-charge-entangled double quantum dot, *Nat. Phys.* **10**, 145 (2014).
- [58] M. Leijnse and K. Flensberg, Parity qubits and poor man's Majorana bound states in double quantum dots, *Phys. Rev. B* **86**, 134528 (2012).
- [59] T. I. Ivanov, Coherent tunneling through a double quantum dot coupled to Majorana bound states, *Phys. Rev. B* **96**, 035417 (2017).
- [60] J. D. Cifuentes and L. G. G. V. D. da Silva, Manipulating Majorana zero modes in double quantum dots, *Phys. Rev. B* **100**, 085429 (2019).
- [61] M. J. Rancić, S. Hoffman, C. Schrade, J. Klinovaja, and D. Loss, Entangling spins in double quantum dots and Majorana bound states, *Phys. Rev. B* **99**, 165306 (2019).
- [62] Y.-A. Chen, J.-J. Feng, and Z. Wang, Proposal for probing the Majorana zero modes by testing the Pauli exclusion principle with two quantum dots, *Phys. Lett. A* **384**, 126496 (2020).
- [63] K. G. Wilson, The renormalization group: Critical phenomena and the kondo problem, *Rev. Mod. Phys.* **47**, 773 (1975).
- [64] K. Flensberg, Tunneling characteristics of a chain of Majorana bound states, *Phys. Rev. B* **82**, 180516(R) (2010).
- [65] R. Bulla, T. A. Costi, and T. Pruschke, Numerical renormalization group method for quantum impurity systems, *Rev. Mod. Phys.* **80**, 395 (2008).
- [66] We used the open-access Budapest Flexible DM-NRG code, <http://www.phy.bme.hu/~dmnrg/>; O. Legeza, C. P. Moca, A. I. Tóth, I. Weymann, G. Zaránd, [arXiv:0809.3143](https://arxiv.org/abs/0809.3143) (2008) (unpublished).
- [67] I. Weymann, Finite-temperature spintronic transport through kondo quantum dots: Numerical renormalization group study, *Phys. Rev. B* **83**, 113306 (2011).